Contemporary Mathematics
https://ojs.wiserpub.com/index.php/CM/

Research Article

Observational Constraints on Model with Specific Deceleration Parameter

Aroonkumar Beesham[1,2]

[1]Faculty of Applied and Health Sciences, Mangosuthu University of Technology, Durban, South Africa
[2]National Institute of Theoretical and Computational Sciences (NITheCS), South Africa
E-mail: abeesham@yahoo.com

Received: 30 December 2024; **Revised:** 25 July 2025; **Accepted:** 28 July 2025

Abstract: We place observational constraints on a cosmological model with a specific deceleration parameter that depends on the scale factor that has been discussed recently. This form of the deceleration parameter has been discussed by authors in several papers, but none of them have applied observations to constrain the variables of the model. We carry this out with the cosmic chronometer, supernovae and the baryon acoustic oscillation datasets. Use is made of Markov Chain Monte Carlo analysis which implements Bayesian methods in cosmology. This is used to obtain the optimum values for the relevant parameters, which are then used to plot the kinematical and physical parameters of the model. We discuss the verious cosmographic parameters of the model, such as the deceleration and state-finder parameters. There are several issues with any cosmological model based on this deceleration parameter concerning the values of some of the parameters. The transition redshift of the model and the current value of the deceleration parameter do not match with the Planck data. Thus the model does not seem viable.

***Keywords*:** cosmology, dark energy, accelerated expansion of universe, observational constraints, specific deceleration parameter

MSC: 83F05

1. Introduction

The deceleration parameter q in cosmology is defined as:

$$q = -\frac{\ddot{a}a}{\dot{a}^2} \tag{1}$$

where a is the scale factor, and a dot denotes a time derivative. This parameter indicates whether the universe is accelerating or decelerating. A positive value of q means deceleration, and a negative value acceleration. This notation stems from historical reasons, when the universe was believed to be decelerating. If $q = 0$, then there is no acceleration, and the universe is expanding at a constant rate.

DOI: https://doi.org/10.37256/cm.6520256325

Observations indicate that the universe was decelerating in the past, but that, as from a certain time onwards, the universe started accelerating [1, 2]. Cosmology has to be able to explain this. The standard Lambda Cold Dark Matter (ΛCDM) model in general relativity has the most support amongst the community to explain the current acceleration. In this model, the existence of some hypothetical matter with negative pressure is postulated. This exotic matter causes the present acceleration. However, the model has several shortcomings [3, 4], such as the cosmic coincidence and cosmological constant problems. Hence, there is a strong motivation to study modified gravity theories with a view towards explaining the transition, as well as solving some of the problems of the ΛCDM model. Many modified theories possess solutions with late time acceleration without exotic matter that has negative pressure. However, there are situations when, to get solutions, researchers in the field have to make a choice for some parameter, such as the deceleration parameter, Hubble parameter, scale factor, or equation of state parameter.

In this work, we investigate a specific choice of the form of the deceleration parameter q, viz.,

$$q = -1 + \frac{\eta}{1 + a^{\eta}}. \tag{2}$$

where $\eta > 0$ is a positive constant. One very obvious motivation for this is that at late times, for large scale factor a (assuming that for the model, the scale factor a is increasing at late times. This may not always be the case, e.g., for oscillating models), the deceleration parameter q tends to -1, the value for the ΛCDM model at late times. Hence the assumption of this condition ensures that the model will approach the ΛCDM model in future, or equivalently, for large a. Another motivation is that, as we shall see later in detail, it has only two parameters that need to be constrained by observations. We shall give more motivation at a later stage.

We first describe briefly the models in the literature with this form of the deceleration parameter q. Singha and Debnath [5] investigated a quintessential cosmological model, with a minimally coupled scalar field, assuming the form (2) of the deceleration parameter q. A barotropic fluid and models dominated by Chaplygin gas provide a transition from deceleration to acceleration. For this, the potential function $V(\phi)$ is always decreasing with the scalar field ϕ. The behaviour of the models at different stages during their evolution was illustrated by plots of the statefinder parameters (r, s) (these parameters will be defined later).

Bali and Singh [6] studied a Bianchi I model with bulk viscosity and variable cosmological parameter. They assumed a relationship of the form $H(a) \equiv \dot{a}/a = \zeta(a^n + 1)$, where $\zeta > 0$ is a constant. This form is equivalent to equation (2). They found that they get a transition from deceleration to acceleration, a decreasing cosmological parameter, and that the model tends to the de-Sitter stage at late times (exponential expansion as for the ΛCDM model), becoming isotropic. These authors, inter alia, only worked with cosmic time t instead of the redshift z, did not apply any observational constraints, did not provide any figures, and apart from the deceleration parameter, did not work out any of the other cosmographic parameters.

Chirde and Shekh [7] investigated a symmetric plane non-static space-time in $f(R, T)$ gravity containing a perfect fluid, with R being the Ricci Scalar, and T the trace of the energy-momentum tensor T_{ab}. In order to get a specific solution, a special form of q as in (2) was used. The other relation that was assumed was that the equation of state parameter and the metric potentials are proportional to the skewness parameter. The anisotropy initially increases, reaching a maximum at some finite time, and then decreases to zero in keeping with current observations. For $n \geq 1$, the model initially decelerates, and then later accelerates. Some kinematical and physical properties of the model was also studied.

The study of the spatially homogeneous and anisotropic Bianchi type-I universe in $f(R, T)$ gravity was undertaken by Sahoo et al. [8]. They assumed two different forms of $f(R, T)$, viz., $f(R, T) = f_2(T) + f_1(R)$ and $f(R, T) = 2f(T) + R$ and and incorporated bulk viscosity. A form (2) of the deceleration parameter was employed. Exact solutions of the field equations were found, and the kinematical and physical properties of both sets of models were studied in detail as far as the future of the universe as concerned. The nature of the weak, dominant and strong energy conditions for both cases were investigated. The analysis revealed that both models incorporating a bulk viscosity matter component

exhibit an acceleration of the universe during late times. Furthermore, the cosmic jerk parameter aligns well with the three kinematical data sets. All energy conditions were also investigated.

Recently, Pawde et al. [9] conducted an investigation into an anisotropic model within the framework of $f(R, L_m)$ gravity where L_m is the matter Lagrangian. They adopted the specific form $f(R, L_m) = R^2 + L_m^{\alpha} + \beta$, where β represents a constant. This study focused on elucidating the dynamics of the universe by examining a variable deceleration parameter of the type (2). Furthermore, the researchers employed energy conditions, jerk, equation of state, and state-finder parameters to enhance the understanding of the evolution of the universe in this modified gravity context. They reported that their results were consistent with recent observational data and aligned with the ΛCDM model. However, it is noteworthy that no observational diagrams depicting cosmic chronometer, supernovae or baryon acoustic background data were included, nor was any Markov Chain Monte Carlo (MCMC) analysis carried out.

In this investigation, we constrain the parameters of the model studied in ref. [9] by utilising observations. This is the major motivation for the choice of deceleration parameter as in equation (2). We carry this out with the cosmic chronometer, supernovae and baryon acoustic datasets. The optimum values for the relevant variables are found, as opposed to the ad hoc choices that Pawde et al. [9] made. We plot the kinematic parameters of the model, such as the state-finder parameters (r, s), jerk parameter j, and deceleration parameter q. Whilst the model does exhibit a transition from deceleration to acceleration, we find that this model as in [9] is not viable as it does not satisfy observational constraints.

2. Kinematic quantities

We first discuss the kinematical quantities associated with the choice of function for q as in equation (2). The Hubble parameter $H(a)$ is defined as $H(a) \equiv \dot{a}/a$, where a is the scale factor (or as is sometimes called the radius of the universe). Since H is essentially the derivative of the scale factor, a positive value of H indicates expansion of the universe, and a negative value, contraction. A zero value indicates no expansion or contraction, i.e., a static universe. From equation (2), the Hubble parameter can be obtained as:

$$H(a) \equiv \frac{\dot{a}}{a} = \xi(1 + a^{\eta}) \tag{3}$$

where ξ is an integration constant. The scale factor $a(t)$ as a function of time t can be calculated from $H = \dot{a}/a$:

$$a(t) = (e^{\eta t} - 1)^{1/\eta} \tag{4}$$

Now the redshift z in terms of a is given by:

$$a = (1 + z)^{-1} \tag{5}$$

where z is the redshift. The redshift z is an alternative to the time t, and has advantages when discussing observations and observational constraints. It should be noted that an increase of time is accompanied by a decrease in the redshift z, with $z = 0$ referring to the present time. Hence, we find the Hubble parameter in terms of redshift from equations (2), (3)-(5) as:

$$H = \frac{H_0}{2}[1 + (1 + z)^{\eta}]. \tag{6}$$

where H_0 is the current value of the Hubble parameter. The deceleration parameter in terms of redshift from equations (2) and (5) is given by:

$$q(z) = q = -1 + \frac{\eta}{1+(1+z)^{-\eta}} \tag{7}$$

We now provide additional motivation for our choice of deceleration parameter q as in equation (7). The study of cosmological models within the climate of late time acceleration relies heavily on kinematic variables. The deceleration parameter, e.g., characterizes the behavior of the universe, such as whether it is undergoing deceleration, acceleration, or in a transition phase.

The motivation behind a parametrization of the deceleration parameter comes from the fact that the deceleration parameter is an important cosmological parameter that characterizes the dynamics of the universe. It is defined as the ratio of the cosmic acceleration to the cosmic expansion rate, i.e., $q = -\ddot{a}/(aH^2)$. In the past, the deceleration parameter was thought to be constant, indicating that the universe is either slowing down or maintaining a constant rate of expansion. However, observational evidence in recent years suggests that the universe is in fact accelerating at present, which requires a modification of the deceleration parameter. To account for this acceleration, various parametrizations of the deceleration parameter have been proposed in the literature [10] (and references therein). For our choice of q, we can make some qualitative remarks about how q varies with redshift.

• The parameter η relates to the present value of the deceleration parameter, i.e., $q_0 = -1 + \eta/2$. The present state of the universe depends upon the value of η. If $\eta = 2$, then $q_0 = 0$, and the universe is undergoing constant expansion. If $\eta > 2$, then $q_0 > 0$, and we have decelerated expansion. Finally, if $0 < \eta < 2$, then $q_0 < 0$, and we have accelerated expansion.

• In the distant past, $z >> 1$, and $q(z) \to -1 + \eta$. For $\eta > 1$, we have $q > 0 \implies$ deceleration, i.e., the radiation and matter dominated eras.

• In the far future, from the form of $q(a)$ as in equation (2), and the discussion following that equation, we have seen that $q \to -1$, the asymptotic form for q for the ΛCDM model. Hence this model will asymptotically approach the ΛCDM model in future.

3. Observational constraints

In this section, a statistical analysis is performed to compare the predictions of the theoretical model with observational data. The goal is to establish constraints on the free parameters of the model, namely H_0 and η. Some more recent studies that discuss advances in observational constraints are Sudharani et al. [11], Pawar et al. [12], Pawar and Mapari [13], Pawar et al. [14].

The Cosmic Chronometer (CC), Type Ia Supernovae (SNIa) (Pantheon), and the Baryonic Acoustic Oscillations (BAO) datasets are used. The first two datasets are made up of 31 and 1,048 data points, respectively. A software package in Python [15] is used, implementing MCMC analysis which implements Bayesian methods in cosmology [16]. To estimate the posterior distribution of the model parameters, the MCMC sampler is used. Multiple iterations of MCMC sampling are used to compute the posterior distribution, and observational data is used to construct the likelihood function. To get the best-fitting results, we use 1,000 steps and 100 walkers in our MCMC analysis. The likelihood function is [17, 18]:

$$L \propto \exp(-\chi^2/2) \tag{8}$$

where the pseudo chi-squared function is given by χ^2 [16]. This seems to be the most common likelihood function L used by observational cosmologists, and hence we have adopted this form. The motivation for this particular form is the following. The formula for the probability density function for a normal distribution contains the term. So when one takes the log of that function, it becomes just the usual $-\chi^2/2$. Now in basic MCMC analysis, we want to calculate the posterior probability function, which is nothing but usually a joint probability function for a normal distribution case. So in this case, the posterior probability for the joint case becomes $\exp[-\sum(-\chi^2/2)]$. Now we have to find the maximum of this posterior probability. So for ease of calculation, we calculate the maximum of log (Posterior), which simply becomes a $(-\chi^2/2)$ function. Now these two optimization problems, viz., firstly to calculate the maximum of the log (Posterior), and secondly, the minimum of of $(-\chi^2/2)$ become equivalent. So the expression $\exp(-\chi^2/2)$ is due to the normal distribution, and we take the log of the Likelihood to make thins simpler. Given a particular L, it is sometimes easier to rewrite the likelihood as the log of the likelihood. This entails no loss of generality as maximizing a log likelihood is the same as maximizing a likelihood. There are several other likelihood functions and methods that can potentially be used, but many of them are still in the trial/developmental phase. Some of these are machine learning emulators [19], partition function approach [20], renormalisation group computation [21], principal component analysis [22], Copula method (should yield a more accurate likelihood function in future [23, 24]).

Bayesian parameter estimation involves exploring the parameter space θ, often with algorithms like Metropolis-Hastings [25], which helps guide a random walker through the space, preferring regions with higher likelihoods. The mean and uncertainty of each parameter are usually found by analyzing where the walker spends most of its time and how far it deviates within the parameter space. In situations where we have a nearly Gaussian posterior distribution, information criteria offers a simpler approach to model selection [26]. In this work, we investigate the form (2) for the deceleration parameter. A MCMC analysis with the emcee package [27] is used to properly cover the parameter space in order to get reliable estimates. The GetDist package [28] is employed to visualize and plot the posterior distributions. This enables the proper determination of contraints for the parameters. The analysis was performed with 30 walkers and 30,000 iteration, allowing efficient sampling of the parameter space. The prior distributions were chosen based on observational constraints and set as: $H_0 \in [50, 100]$ km/s/Mpc and $\eta \in [0, 4]$. These priors ensure a broad but physically meaningful parameter exploration while preventing over-restriction of the search space. The GetDist package [29] is employed to visualize and plot the posterior distributions and the 1σ and 2σ confidence intervals for each parameter are presented in Table 1. The likelihood function was constructed by summing the χ^2 contributions from each dataset, ensuring a robust and unbiased estimation of cosmological parameters. To ensure consistency and reliability, the datasets were combined without additional weighting, treating each dataset equally in the likelihood function. This approach prevents any individual dataset from disproportionately influencing the constraints, thereby providing a well-balanced parameter estimation. The convergence of the MCMC chains was assessed by analyzing the posterior distributions and verifying that the results remained stable over multiple runs. Convergence was checked using Gelman-Rubin statistics.

The selection of observational datasets in this study was motivated by their complementary roles in constraining different aspects of cosmic expansion (For the latest datasets that we used, we refer to the recent preprint by Du et al. [30] who give a very comprehensive review of all the datasets, including Dark Energy Spectroscopic Instrument (DESI)). CC provide a direct, model-independent measurement of $H(z)$ based on galaxy age estimates, making them essential for tracking the universe's expansion history. SNIa-Pantheon+ data, on the other hand, offer precise luminosity distance measurements, playing a crucial role in constraining the equation of state of dark energy and the deceleration parameter $q(z)$. Finally, BAO serve as a standard ruler, allowing precise constraints on the Hubble constant H_0. The combination of these datasets ensures that the parameter constraints obtained in this study are independent, robust, and cross-validated.

By utilizing these three independent probes, we mitigate potential biases that might arise from relying on a single dataset. This approach enables a more comprehensive analysis of cosmic acceleration and dark energy evolution.

3.1 *Observational H(z) data*

By measuring the relative ages of galaxies that are passively evolving, the CC dataset can estimate the Hubble parameter. Galaxies can be recognized by certain characteristics in their color profiles and spectra [31]. CC get their data from the estimated ages of galaxies at different redshifts. Use is made of the 31 independent $H(z)$ observations in

the redshift range $0.07 \leq z \leq 2.41$ in the analysis [32]. The formula $H(z) = -\frac{1}{1+z}\frac{dz}{dt}$ is used to acquire these $H(z)$ measurements. In this case, $\frac{dz}{dt}$ is taken as $\frac{\Delta z}{\Delta t}$, where Δz and Δt indicate the different redshifts and corresponding ages of two galaxies. Then the corresponding χ^2 function is:

$$\chi^2_{Hz} = \sum_{k=1}^{31} \frac{[H_{\text{th}}(z_i) - H_{\text{obs},\,i}]^2}{\sigma_i^2}. \tag{9}$$

where

- $\mu_{\text{obs},\,i}$ is the observed distance modulus of the i-th object,
- $\mu_{\text{th},\,i}$ is the theoretical distance modulus predicted by the cosmological model,
- σ_i is the uncertainty in the observed distance modulus.

The best-fit values of the model parameters are obtained by minimizing the chi-square statistic χ^2. This is illustrated in Figure 1 corresponding to the 1σ and 2σ error bars obtained from the CC data. The best-fit values of the model parameters are obtained by minimizing the chi-square statistic χ^2. This is illustrated in Figure 1 corresponding to the 1σ and 2σ error bars obtained from the CC data.

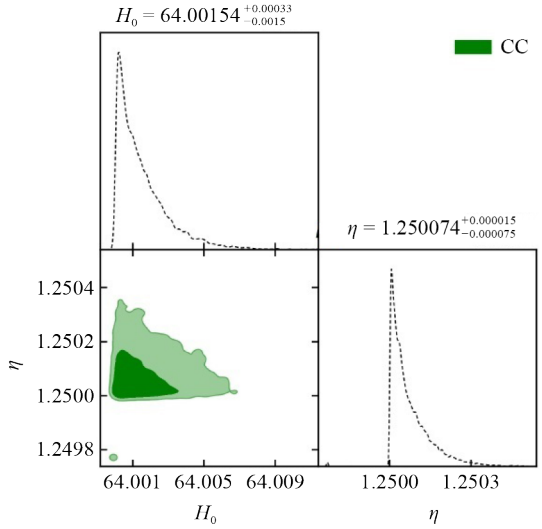

Figure 1. This figure corresponds to 1σ and 2σ error bars obtained from CC data

3.2 *Pantheon dataset and observational constraints*

The Pantheon dataset is a comprehensive compilation of 1,048 Type Ia Supernovae (SNIa) observations over a redshift range of $0.01 < z < 2.3$. It is widely used to constrain cosmological parameters and test various cosmological models, including the standard ΛCDM model and models in modified theories of gravity. The key observable in the Pantheon dataset is the *distance modulus* $\mu(z)$, which is related to the luminosity distance $d_L(z)$ by:

$$\mu(z) = 5\log_{10}\left[\frac{d_L(z)}{1\ Mpc}\right] + 25, \tag{10}$$

where $d_L(z)$ is the luminosity distance in Megaparsecs (Mpc). The luminosity distance depends on the cosmological model and is given by:

$$d_L(z) = (1+z)\int_0^z \frac{dz'}{H(z')} \tag{11}$$

where z' is an arbitrary variable of integration and $H(z')$ is the Hubble parameter.

Again we minimize the chi-square statistic to obtain the best-fit values of the model parameters:

$$\chi^2_{\text{SNIa}} = \sum_{i=1}^{N} \frac{[\mu_{\text{obs},\,i} - \mu_{\text{th},\,i}]^2}{\sigma_i^2}, \tag{12}$$

The best-fit parameters (H_0, n) are those that minimize χ^2, yielding the maximum likelihood estimate of the parameters. In Figure 2, the likelihood contours at 1σ and 2σ levels for the Pantheon data are illustrated. We have illustrated only the Pantheon data, and not the CC + SNIa data, as the values for this, for some reason or the other, were very close to those of the CC dataset.

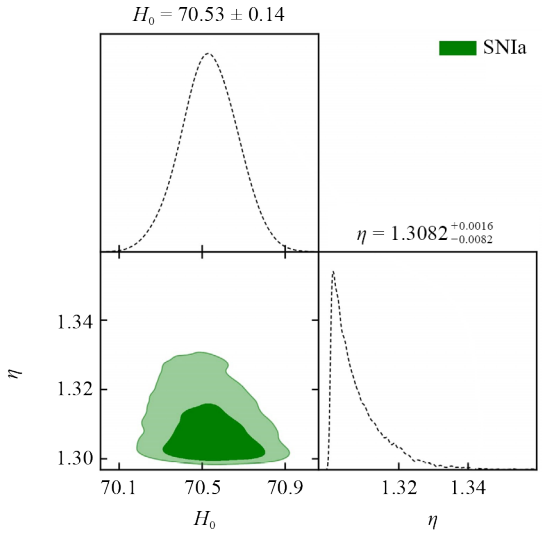

Figure 2. This figure corresponds to 1σ and 2σ error bars obtained from SNIa datasets

3.3 *BAO datasets*

BAOs are pressure waves produced by cosmological perturbations in the baryon-photon plasma during the recombination epoch, appearing as distinct peaks on large angular scales. In this study, we utilize the 26 BAO dataset points from the six degree Field Galaxy Survey (6dFGS), the Sloan Digital Sky Survey (SDSS), and the Low-Redshift Galaxy (LOWZ) samples of the Baryon Oscillation Spectroscopic Survey (BOSS) [33]. The surveys have provided highly accurate measurements of the positions of the BAO peaks in galaxy clustering at different redshifts. The dilation scale, $D_v(z)$ is given by

$$D_v(z) = \left[\frac{d_A^2(z), cz}{H(z)}\right]^{1/3}, \tag{13}$$

where $d_A^2(z)$ is the angular diameter distance, and c is the sped of light. The chi-square for BAO data, χ^2_{BAO}, is expressed as

$$\chi^2_{\text{BAO}} = \mathbf{X}^{\text{T}}\mathbf{C}^{-1}\mathbf{X}, \tag{14}$$

where the vector $\mathbf{X}$ is the ratio of the luminosity distance $d_A(z)$ to the dilaton scale D_V, and $\mathbf{C}$ denotes the covariance matrix [34].

3.4 *Hz + SNIa + BAO datasets*

In addition, use is made of χ^2_{total} in order to get, from the combined $H(z)$, Pantheon+ and BAO data, constraints on the parameters H_0, and η. So, the definition of the required chi-square function is:

$$\chi^2_{\text{total}} = \chi^2_{Hz} + \chi^2_{\text{SNIa}} + \chi^2_{\text{BAO}} \tag{15}$$

Gaussian priors are used as follows for analysing: $[1, 5]$ for η, and $[60, 80]$ for H_0. For the CC data, SNIa and CC + SNIa + BAO data, the corresponding $1-\sigma$ and $2-\sigma$ contour plots, are shown in Figures 1, 2, and 3, respectively.

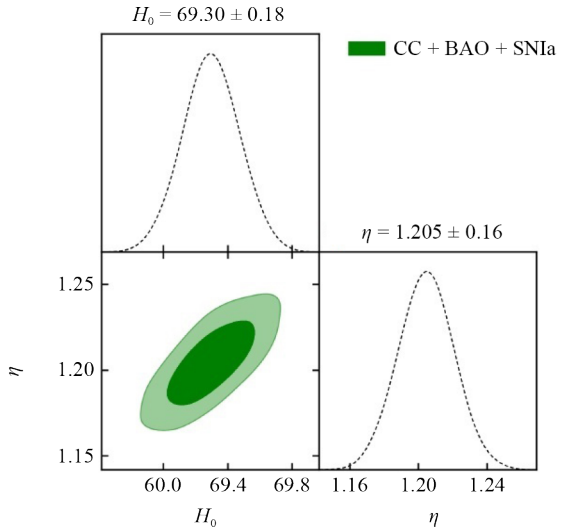

Figure 3. This figure corresponds to 1σ and 2σ error bars obtained from CC + SNIA + BAO data

With 68% confidence limit, the results are as follows: $H_0 = 64.00$ and $\eta = 1.25$, for the CC data; $H_0 = 70.54 \pm 0.14$ and $\eta = 1.3082^{+0.0016}_{-0.0081}$ for the SNIa data; $H_0 = 69.30 \pm 0.02$ and $\eta = 1.20 \pm 0.02$, for the CC + SNIa + BAO data. We note that the values that Pawde et al. [9] have used for η are 1.4, 1.6 and 1.8, which are somewhat outside the values as obtained from observations.

In the Table 1 below, we display all our values for the different datasets:

Table 1. Values of parameters for different datasets

Parameters	CC dataset	SNIa dataset	CC + BAO + SNIa dataset
H_0	64.00	70.54 ± 0.14	69.30 ± 0.02
η	1.25	$1.3082^{+0.0016}_{-0.0081}$	1.20 ± 0.02

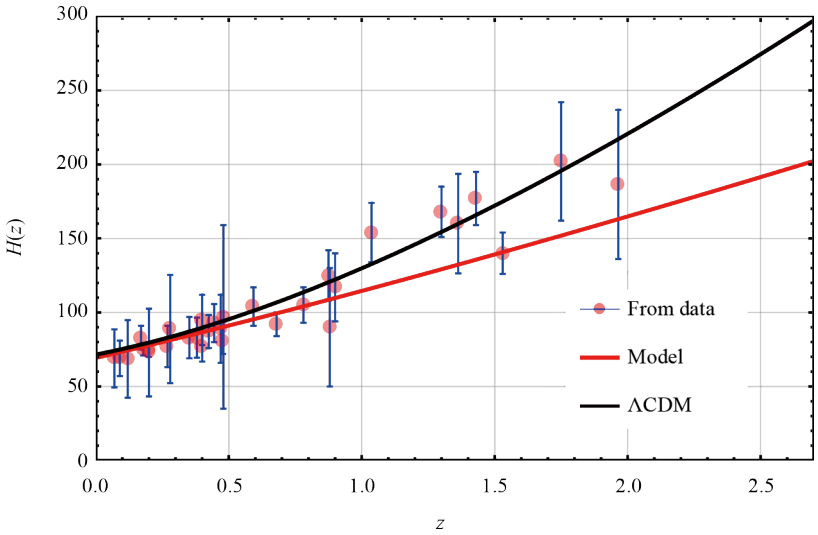

Figure 4. This figure displays the $H(z)$ curve using CC + SNIa + BAO data with error bars indicated

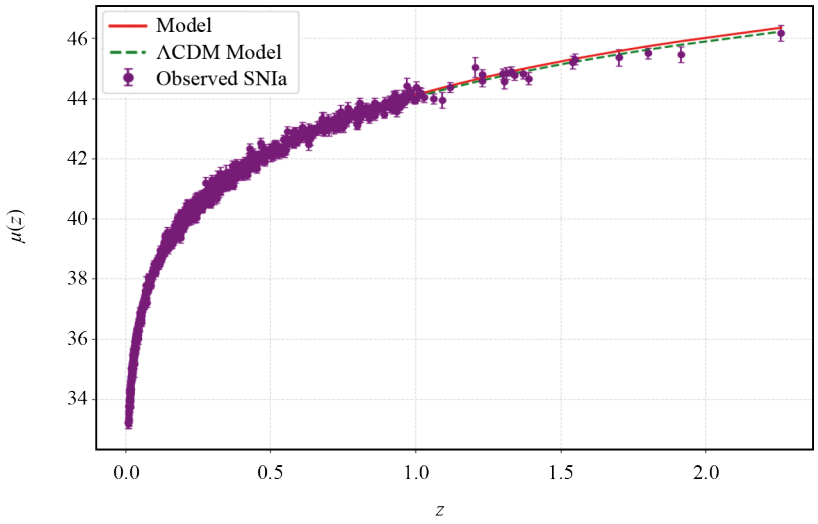

Figure 5. This figure displays the $\mu(z)$ curve using CC + SNIa + BAO data, with error bars indicated

In Figure 4, we have displayed the $H(z)$ curve using the CC + SNIa + BAO dataset, which shows the close correspondence between the ΛCDM model and our data. At present, the data for both the models converge, but as we go back into the past, the curves tend to diverge. This is due to the different dependencies for both models, with the $H(z)$ for the ΛCDM model varying as $(1+z)^{1.5}$, whereas our model varies as $(1+z)^{1.2}$ for the combined CC + SNIa + BAO dataset. Figure 5 shows the $\mu(z)$ curve using the combined CC + SNIa + BAO data, and once again we see a close relationship with the ΛCDM model. The curves behave similarly as previously described for $H(z)$. This is not surprising, noticing the definition of the distance modulus $\mu(z)$ in equation (10), together with equation (11).

4. Cosmographic parameters

Cosmography is an important branch of cosmology for which a description of the universe is sought independently of any cosmological model [35–41], and references therein. One expands a suitable parameter, such as the equation of state parameter, deceleration parameter, Hubble parameter, or scale factor, in a Taylor series around the current time. This enables comparing these quantities with observational data. So, cosmography is a technique which, in a certain sense, is independent of any specific cosmological model. It may be utilised to match parameters with observational constraints. However, there are some limitations on its use as far as re-constructions of models are concerned. The easiest parameter to use for expansion in a Taylor series is the scale factor. The terms of the Taylor series can be compared to various cosmographic parameters as follows:

$$H \equiv \frac{1}{a}\frac{da}{dt}, \quad q \equiv -\frac{1}{aH^2}\frac{d^2a}{dt^2}, \quad j \equiv r \equiv \frac{1}{aH^3}\frac{d^3a}{dt^3}, \tag{16}$$

$$s \equiv \frac{1}{aH^4}\frac{d^4a}{dt^4}, \quad l \equiv \frac{1}{aH^5}\frac{d^5a}{dt^5}, \quad m \equiv \frac{1}{aH^6}\frac{d^6a}{dt^6} \ etc. \tag{17}$$

where j (or also called r) is the jerk parameter (or jolt), s the snap (or facetiously called jounce), l the lerk (or facetiously called crackle) and m the pop parameter. Less common alternative names for the j parameter are pulse, impulse, bounce, surge, shock and super-acceleration.

We now discuss these parameters in more detail. The jerk parameter indicates the rate of change of the deceleration parameter. A positive j refers to an increase in q, and a negative q a decrease. The standard ΛCDM model has a constant j given by $j = 1$. Generally other models/theories have a changing j indicating a change in the dynamics of those models/theories. Now before the parameters above the Hubble and deceleration were introduced, Sahni et al. [42] came up with the concept of a diagnostic pair. This was motivated by the necessity of consideration of more general models of dark energy than just a cosmological constant and the remarkable increase in the accuracy of cosmological observational data during the last few years. This compelled them to advance beyond just H and q. For this reason, a new geometrical diagnostic pair for dark energy was introduced. This diagnostic pair was constructed from the third order derivative of the scale factor, and can successfully differentiate between various different dark energy models, hence its importance. The pair (r, q) can also serve the same purpose. A few more recent references on statefinder studies are Patil et al. [43, 44]. The lerk and pop parameters are given just for convenience, but are not used further.

We now plot several of these parameters using $\eta = 1.20$ from the combined data, and compare with the ΛCDM model. For all subsequent Figures, we use this value for $\eta = 1.20$. The other values for η do not make much of a difference to the picture.

Firstly, in Figure 6, we plot the deceleration parameter against redshift using the combined data value $\eta = 1.20$. From equation (7), we see that the current value of the deceleration parameter q is $q(0) = -0.38$, using the value $\eta = 1.25$ (from the CC data). The transition redshift z_t, i.e., the redshift z_t for which the universe changes from deceleration to acceleration, is given by $q(z_t) = 0$, from which we get $z_t = 2.03$. For the SNIa dataset, $\eta = 1.31$, we get $q(0) = -0.345$, $z_t = 1.44$. For

$\eta = 1.20$ from the CC + SNIa + BAO data, we get $q(0) = -0.40$ and $z_t = 2.82$. The ΛCDM model has $q(0) \sim -0.55$, $z_t = \left[\frac{2(1-\Omega_{\Lambda 0})}{\Omega_{m0}}\right]^{(1/3)} - 1 = 0.67$ using the Planck 2018 data [45]. The values obtained with the present choice of deceleration prameter q in this model are higher than the ΛCDM model for $q(0)$, and much higher for the transition redshift z_t. They do not match, indicating that the present model is not viable. This is a very serious problem with the model of Pawde [9].

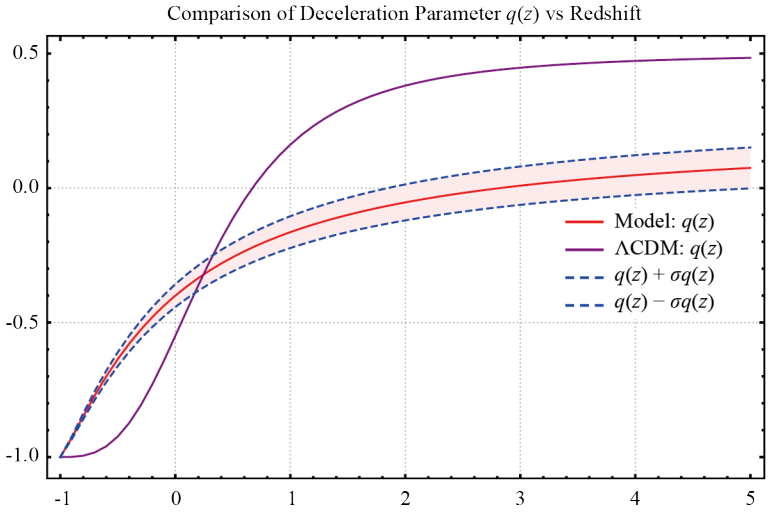

Figure 6. Deceleration parameter q vs redshift z for the combined CC + SNIa + BAO dataset with error bars shaded. q on Y-axis, z on X-axis

The jerk parameter is given by

$$j = 1 + \frac{\eta^2}{\left(\frac{1}{1+z}\right)^{\eta} + 1} + \frac{\eta^2}{\left(\left(\frac{1}{1+z}\right)^{\eta} + 1\right)^2} - \frac{3\eta}{\left(\frac{1}{1+z}\right)^{\eta} + 1} \tag{18}$$

The snap parameter is given by

$$s = \frac{2\eta^2\left(\left(\frac{1}{1+z}\right)^{\eta} + 1\right) - 6\eta}{6\eta - 9\left(\left(\frac{1}{1+z}\right)^{\eta} + 1\right)} \tag{19}$$

The evolution of the $r-q$ curve is given in Figure 7 (note that the formula for r is the same as that of j). The curve does not continue just after $q > 0$. This is due to a singularity at that point, and this is also reflected in the corresponding figure of Pawde et al. [9]. For clarity we point out the in Figures 7 and 8, the region above the line $r = 1$ is the Chaplygin gas region, and the region below that line is the quintessence region.

In Figure 8, we have illustrated the (r, s) state-finder parameter curve. In Figures 6-8, we used the CC + SNIa + BAO data to plot the curves.

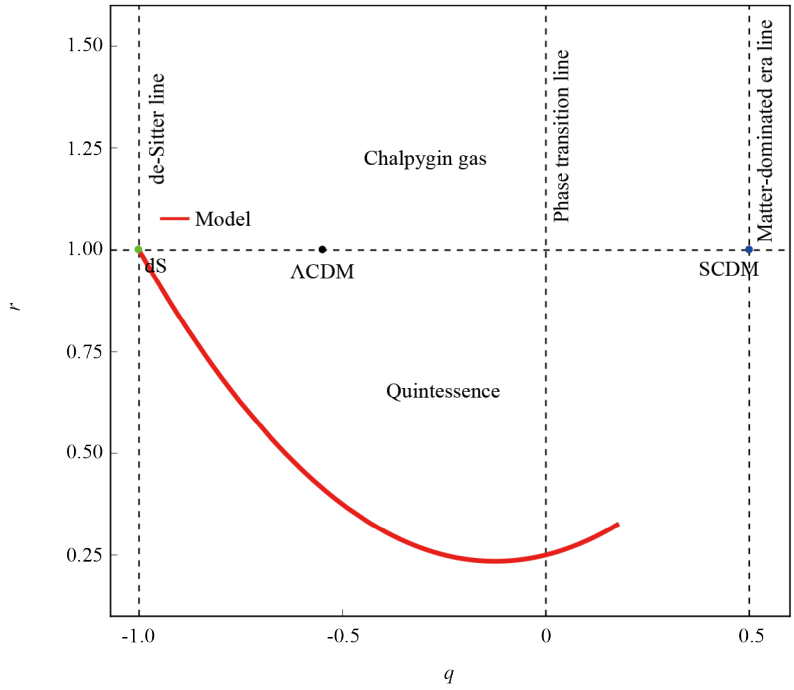

Figure 7. State-finder parameter r against deceleration parameter q for the CC + SNIa + BAO dataset

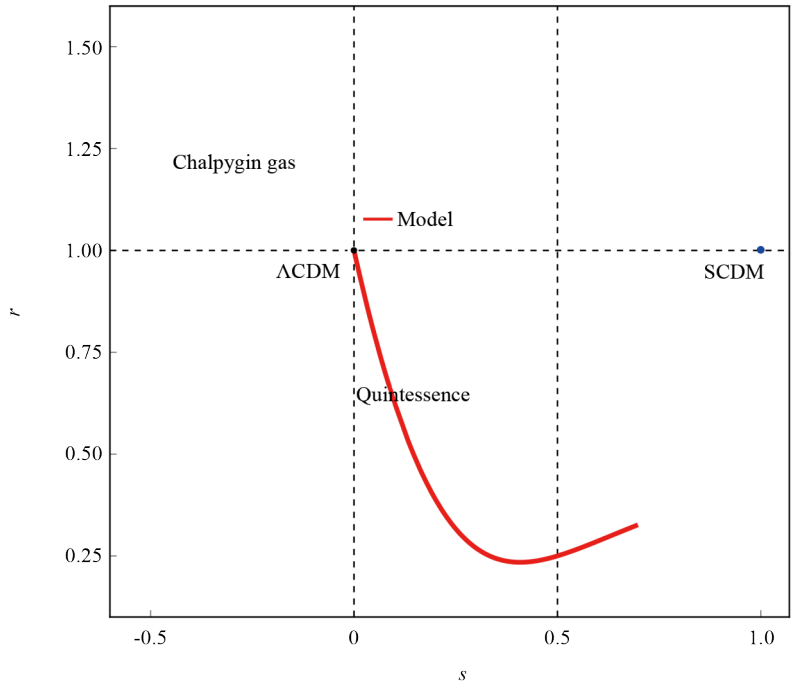

Figure 8. State-finder parameter (r, s) curve for the CC + SNIa + BAO dataset

5. Discussion

In this work, we have applied observational constraints to the model discussed by Pawde et al. [9] in $f(R, L_m)$ gravity. These authors chose a particular form for the deceleration parameter of the form equation (1). Those authors did not apply observational constraints to determine the parameter η of the model, but rather chose values of η equal to 1.4, 1.6 and 1.8, respectively. One needs to apply observational constraints to determine η. This is the major issue with the model. We have applied observational constraints from CC, SNIa, and BAO datasets to determine η. We find that $\eta = 1.25$ for the CC dataset, 1.31 for the SNIa dataset, and 1.2 for the combined CC + SNIa + BAO datasets. The values of [9] are somewhat higher than the above-mentioned. Their current values for the deceleration parameter, viz., -0.11, -0.21 and -0.32 as well as the transition redshift, viz., 0.92, 0.4 and 0.15 do not match with those of the ΛCDM model -0.55 and 0.67, respectively, and this presents a serious problem for the model studied here.

We began by giving some background in the introduction to the particular form of q. Then in section 2, we discussed the basic formalism of $f(R, L_m)$ gravity. Then in section 3, we studied the Locally Rotationally Symmetric (LRS) Bianchi I metric in the theory, giving the field equations. Then we choose the required form for $f(R, L_m)$ gravity in section 4. In section 5, we gave the forms for the scale factor a, Hubble parameter H and q both in terms of the time t and redshift z. A detailed motivation for the chosen parametrization of $q(z)$ was given.

The next section deals with the observational constraints that we find using the CC, SNIa and the combined CC + SNIa + BAO datasets. Best fit values for the present Hubble parameter H_0 and the parameter η were determined. We then plotted the $H(z)$ and $\mu(z)$ graphs in Figures 4 and 5, respectively. For subsequent analysis, we chose the value $\eta = 1.20$ from the combined set (the other values do not affect the picture to any large extent). We have plotted curves of the relevant cosmographic parameters q, (r, q), and (r, s) in Figures 6-8. These Figures show how the model differs from the ΛCDM model, and also gives some idea of how the model evolves. Some other relevant references are [46–48].

In conclusion, we can say that the present model of Pawde et al. [9] and choice of deceleration parameter q does not fit in with observational constraints. However, the model does possess many positive attributes, e.g., its simplicity. It does have a transition from deceleration to acceleration. Those authors gave an excellent analysis of the form (19) of the deceleration parameter and its properties. Beautiful color figures were drawn of the scale factor, Hubble parameter, deceleration parameter and several statefinder parameters. In addition a complete application to the Bianchi I model in $f(R, L_m)$ gravity was provided, including an analysis of the equation of state. They showed how the different phases of the evolution of the universe could be obtained. We are currently attempting to determine how to modify the choice of q so that a better model could be obtained. Most likely, the reason for this could be that there is only one parameter in the model (apart from the current Hubble parameter), and perhaps one needs more than one parameter. We are currently investigating this possibility, e.g., including a parameter ν in q as follows: $q = -1 + \dfrac{\eta}{1+a^{\nu}}$, or even two additional parameters, $q = -1 + \dfrac{\eta}{1+\zeta a^{\nu}}$. Then one could run through the entire observational analysis as we carried out in this paper to determine if better models could be obtained. If so, then an application to a specific theory can be done. We and hope to report on the result soon.

Acknowledgement

The author sincerely thanks the reviewers for their detailed comments which have led to a substantial improvement in the manuscript. In addition, the author acknowledges Dr. Bhupendra Kumar Shukla for his useful comments.

Conflict of interest

The author declares no competing financial interest.

References

[1] Riess AG, Filippenko AV, Challis P, Clocchiatti A, Diercks A, Garnavich PM, et al. Observational evidence from supernovae for an accelerating universe and a cosmological constant. *Astronomical Journal*. 1998; 116: 1009. Available from: https://doi.org/10.1086/300499.

[2] Perlmutter S, Aldering G, Goldhaber G, Knop RA, Nugent P, Castro PG, et al. Measurements of Ω and Λ from 42 high-redshift supernovae. *Astrophysical Journal*. 1999; 517: 565. Available from: https://doi.org/10.1086/307221.

[3] Durrer R, Maartens R. Dark energy and dark gravity: Theory overview. *General Relativity and Gravitation*. 2008; 40: 301-328. Available from: https://doi.org/10.1007/s10714-007-0549-5.

[4] Abdalla A, Guillermo FA, Aboubrahim A, Agnello A, Akarsu O, Akrami Y, et al. Cosmology intertwined: A review of the particle physics, astrophysics, and cosmology associated with the cosmological tensions and anomalies. *Journal of High Energy Astrophysics*. 2022; 34: 49-211. Available from: https://doi.org/10.1016/j.jheap.2022.04.002.

[5] Singha AK, Debnath U. Accelerating universe with a special form of decelerating parameter. *International Journal of Theoretical Physics*. 2009; 48: 351-356. Available from: https://doi.org/10.1007/s10773-008-9807-x.

[6] Bali R, Singh P. Bulk Viscous Bianchi type I barotropic fluid cosmological model with varying Λ and functional relation on Hubble parameter. *International Journal of Theoretical Physics*. 2012; 51: 772-777.

[7] Chirde VR, Shekh SH. Dark energy cosmological model in a modified theory of gravity. *Astrophysics*. 2015; 58: 106-119. Available from: https://doi.org/10.1007/s10511-015-9369-6.

[8] Sahoo PK, Parbati Sahoo P, Bishi BK. Anisotropic cosmological models in $f(R, T)$ gravity with variable deceleration parameter. *International Journal of Geometric Methods in Modern Physics*. 2017; 14: 1750097. Available from: https://doi.org/10.1142/S0219887817500979.

[9] Pawde J, Mapari R, Patil V, Dnyaneshwar D. Anisotropic behavior of universe in $f(R, L_m)$ gravity with varying deceleration parameter. *European Physical Journal C*. 2024; 84: 320. Available from: https://doi.org/10.1140/epjc/s10052-024-12646-4.

[10] Koussour M, Myrzakulov N, Alfedeel AHA, Awad F, Bennai M. Modeling cosmic acceleration with a generalized varying deceleration parameter. *Physics of the Dark Universe*. 2023; 42: 101339. Available from: https://doi.org/10.1016/j.dark.2023.101339.

[11] Sudharani L, Kavya NS, Naik DM, Venkatesha V. Hubble parameter reconstruction: A tool to explore the acceleration of the universe with observational constraints. *Chinese Journal of Physics*. 2023; 85: 250-263. Available from: https://doi.org/10.1016/j.cjph.2023.07.015.

[12] Pawar DD, Gaikwad PS, Muhammad S, Zotos EE. Two fluids in $f(T)$ gravity with observational constraints. *Astronomy and Computing*. 2024; 48: 100863. Available from: https://doi.org/10.1016/j.ascom.2024.100863.

[13] Pawar DD, Mapari RV. Plane symmetry cosmology model of interacting field in $f(R, T)$ theory. *Journal of Dynamical Systems and Geometric Theories*. 2022; 20(1): 115-136. Available from: https://doi.org/10.1080/1726037X.2022.2079268.

[14] Pawar DD, Ghungarwar NG, Muhammad S, Zotos E. Observational constraints on quark and strange quark matters in $f(R, T)$ theory of gravity. *Astronomy and Computing*. 2025; 51: 100924. Available from: https://doi.org/10.1016/j.ascom.2024.100924.

[15] Foreman-Mackey D, Hogg DW, Lang D, Goodman J. Emcee: The MCMC hammer. *Publications of the Astronomical Society of the Pacific*. 2013; 125: 306-312. Available from: https://dx.doi.org/10.1086/670067.

[16] Hobson MP, Jaffe AH, Liddle AR, Mukherjee P, Parkinson D. *Bayesian Methods in Cosmology*. Cambridge: Cambridge University Press; 2009.

[17] Myrzakulov Y, Donmez O, Koussour M, Muminov S, Bekchanov S, Rayimbaev J. Model-independent parameterization of $H(z)$ and its implications for cosmic evolution. *Journal of High Energy Astrophysics*. 2024; 43: 209-216. Available from: https://doi.org/10.1016/j.jheap.2024.07.010.

[18] Errehymy A, Koussour M, Donmez O, Myrzakulov K, Nisar KS, Abdel-Aty AH. Exploring $B(z)$CDM models beyond ΛCDM: Observational data and cosmographic analysis. *Physics of the Dark Universe*. 2024; 46: 101555. Available from: https://doi.org/10.1016/j.dark.2024.101555.

[19] Gong Z, Halder A, Barreira A, Seitz A, Friedrich O. Cosmology from the integrated shear 3-point correlation function: Simulated likelihood analyses with machine-learning emulators. *Journal of Cosmology and Astroparticle Physics*. 2023; 2023(7): 40. Available from: https://dx.doi.org/10.1088/1475-7516/2023/07/040.

[20] Rover L, Bartels LC, Schäfer BM. Partition function approach to non-Gaussian likelihoods: Formalism and expansions for weakly non-Gaussian cosmological inference. *Monthly Notices of the Royal Astronomical Society*. 2023; 523: 2027-2038. Available from: https://doi.org/10.1093/mnras/stad1471.

[21] Donald P. Improved renormalization group computation of likelihood functions for cosmological data sets. *Physical Review D*. 2019; 100: 043511. Available from: https://doi.org/10.1103/PhysRevD.100.043511.

[22] Lin C, Harnois-Deraps J, Eifler T, Pospisil T, Mandelbaum R, Lee AB, et al. Non-Gaussianity in the weak lensing correlation function likelihood—implications for cosmological parameter biases. *Monthly Notices of the Royal Astronomical Society*. 2020; 499: 2977-2993. Available from: https://doi.org/10.1093/mnras/staa2948.

[23] Sato M, Ichiki K, Takeuchi TT. Copula cosmology: Constructing a likelihood function. *Physical Review D*. 2011; 83: 023501. Available from: https://doi.org/10.1103/PhysRevD.83.023501.

[24] Sato M, Ichiki K, Takeuchi TT. Precise estimation of cosmological parameters using a more accurate likelihood function. *Physical Review D*. 2010; 105: 251301. Available from: https://doi.org/10.1103/PhysRevLett.105.251301.

[25] Akeret J, Seehars S, Amara A, Refregier A, Csillaghy A. CosmoHammer: Cosmological parameter estimation with the MCMC Hammer. *Astronomy and Computing*. 2013; 2: 27-39. Available from: https://doi.org/10.1016/j.ascom.2013.06.003.

[26] Bernardo RC, Grandon D, Said JL, Cardenas VH. Parametric and nonparametric methods hint dark energy evolution. *Physics of the Dark Universe*. 2022; 36: 101017. Available from: https://doi.org/10.1016/j.dark.2022.101017.

[27] Hogg DW, Foreman-Mackey D. Data analysis recipes: Using Markov chain Monte Carlo. *arXiv:171006068*. 2017. Available from: https://doi.org/10.48550/arXiv.1710.06068.

[28] Lewis A. GetDist: A python package for analysing Monte Carlo samples. *arXiv:191013970*. 2019. Available from: https://doi.org/10.48550/arXiv.1910.13970.

[29] Stern D, Jimenez R, Verde L, Kamionkowski M, Stanford SA. Cosmic chronometers: Constraining the equation of state of dark energy. *I*: $H(z)$ measurements. *Journal of Cosmology and Astroparticle Physics*. 2010; 2010(2): 8. Available from: https://dx.doi.org/10.1088/1475-7516/2010/02/008.

[30] Du GH, Li TN, Wu PJ, Feng L, Zhou SH, Zhang JF, et al. Cosmological search for sterile neutrinos after DESI 2024. *arXiv:250110785*. 2025. Available from: https://doi.org/10.48550/arXiv.2501.10785.

[31] Moresco M, Jimenez R, Verde L, Cimatti A, Lucia Pozzetti L, Maraston C, et al. Constraining the time evolution of dark energy, curvature and neutrino properties with cosmic chronometers. *Physical Review D*. 2016; 12: 39-62. Available from: https://dx.doi.org/10.1088/1475-7516/2016/12/039.

[32] Solanki R, Pacif SKJ, Abhishek Parida A, Sahoo PK. Cosmic acceleration with bulk viscosity in modified $f(Q)$ gravity. *Physics of the Dark Universe*. 2021; 32: 100820. Available from: https://doi.org/10.1016/j.dark.2021.100820.

[33] Blake C, Brough S, Colless M, Contreras C, Couch W, Croom S, et al. The WiggleZ Dark energy survey: Joint measurements of the expansion and growth history at $z < 1$. *Monthly Notices of the Royal Astronomical Society*. 2012; 425: 405-414. Available from: https://doi.org/10.1111/j.1365-2966.2012.21473.x.

[34] Giostri R, Santos MVD, Waga I, Reis RRR, Calvao MO, Lago BL. From cosmic deceleration to acceleration: New constraints from SN Ia and BAO/CMB. *Journal of Cosmology and Astroparticle Physics*. 2012; 3: 27. Available from: https://dx.doi.org/10.1088/1475-7516/2012/03/027.

[35] visser M. Cosmology without the Einstein equations. *General Relativity and Gravitation*. 2005; 37: 1541-1548. Available from: https://doi.org/10.1007/s10714-005-0134-8.

[36] Bamba K, Capozziello S, Nojiri S, Odintsov SD. Dark energy cosmology: The equivalent description via different theoretical models and cosmography tests. *Astrophysics and Space Science*. 2012; 342: 155-228. Available from: https://doi.org/10.1007/s10509-012-1181-8.

[37] Capozziello S, Agostino R, Luongo O. High-redshift cosmography: Auxiliary variables versus Pade polynomials. *Monthly Notices of the Royal Astronomical Society*. 2020; 494(2): 2576-2590. Available from: https://doi.org/10.1093/mnras/staa871.

[38] Dunsby PKS, Luongo O. On the theory and applications of modern cosmography. *International Journal of Geometric Methods in Modern Physics*. 2016; 13: 1630002. Available from: https://doi.org/10.1142/S0219887816300026.

[39] Vitagliano A, Xia J, Liberati S, Viel M. High-z cosmography at a glance. *arXiv:13027155*. 2013. Available from: https://doi.org/10.48550/arXiv.1302.7155.

[40] Bolotin YL, Cherkaskiy VA, Ivashtenko OY, Konchatnyi MI, Zazunov LG. Applied cosmology: A pegagogical review. *arXiv:181202394*. 2018. Available from: https://doi.org/10.48550/arXiv.1812.02394.

[41] Hu JP, Wang FY. High-redshift cosmography: Application and comparison with different methods. *Astronomy and Astrophysics*. 2022; A71: 1-13. Available from: https://doi.org/10.1051/0004-6361/202142162.

[42] Sahni V, Saini TD, Starobinsky AA, Ujjaini Alam U. Statefinder—a new geometrical diagnostic of dark energy. *Journal of Experimental and Theoretical Physics Letters*. 2003; 77: 201-206. Available from: https://doi.org/10.1134/1.1574831.

[43] Patil V, Pawde J, Mapari R, Waghmare S. FLRW cosmology with hybrid scale factor in $f(R, Lm)$ gravity. *East European Journal of Physics*. 2023; 4: 8-17. Available from: https://doi.org/10.26565/2312-4334-2023-4-01.

[44] Pawar DD, Gaikwad PS, Muhammad S, Zotos EE. Perfect fluid dynamics with observational constraint in the framework of $f(T)$ gravity. *Physics of the Dark Universe*. 2025; 47: 101821. Available from: https://doi.org/10.1016/j.dark.2025.101821.

[45] Aghanim N, Akrami Y, Ashdown M, Aumont J, Baccigalupi C, Ballardini M, et al. Planck 2018 results. VI. Cosmological parameters. *Astronomy and Astrophysics*. 2020; 641: A6. Available from: https://doi.org/10.1051/0004-6361/201833910.

[46] Crighton NHM, Morris SL, Bechtold J, Crain RA, Jannuzi BT, Shone A, et al. Galaxies at a redshift of ~ 0.5 around three closely spaced quasar sightlines. *Monthly Notices of the Royal Astronomical Society*. 2010; 402(2): 1273-1306. Available from: https://doi.org/10.1111/j.1365-2966.2009.15963.x.

[47] Taubenberger S, Suyu SH, Komatsu E, Jee I, Birrer S, Bonvin V, et al. The Hubble constant determined through an inverse distance ladder including quasar time delays and Type Ia Supernovae. *Astronomy and Astrophysics*. 2019; 628: L7. Available from: https://doi.org/10.1051/0004-6361/201935980.

[48] Anukool W, El-Nabulsi RA. An oscillating Chern-Simons universe crossing the phantom divide line and alleviating the Hubble tension. *Modern Physics Letters A*. 2024; 39(17n18): 2450086. Available from: https://doi.org/10.1142/S021773232450086X.